

High-contrast x-ray microtomography in dental research

Graham Davis and David Mills

Queen Mary University of London, Barts & The London School of Medicine and Dentistry,
Institute of Dentistry, London, United Kingdom

ABSTRACT

X-ray microtomography (XMT) is a well-established technique in dental research. The technique has been used extensively to explore the complex morphology of the root canal system, and to qualitatively and quantitatively evaluate root canal instrumentation and filling efficacy in extracted teeth; enabling different techniques to be compared. Densitometric information can be used to identify and map demineralized tissue resulting from tooth decay (caries) and, in extracted teeth, the method can be used to evaluate different methods of excavation. More recently, high contrast XMT is being used to investigate the relationship between external insults to teeth and the pulpal reaction. When such insults occur, fluid may flow through dentinal tubules as a result of cracking or porosity in enamel. Over time, there is an increase in mineralization along the paths of the tubules from the pulp to the damaged region in enamel and this can be visualized using high contrast XMT. The scanner used for this employs time-delay integration to minimize the effects of detector inhomogeneity in order to greatly increase the upper limit on signal-to-noise ratio that can be achieved with long exposure times. When enamel cracks are present in extracted teeth, the presence of these pathways indicates that the cracking occurred prior to extraction. At high contrast, growth lines are occasionally seen in deciduous teeth which may have resulted from periods of maternal illness. Various other anomalies in mineralization resulting from trauma or genetic abnormalities can also be investigated using this technique.

Keywords: high contrast; microtomography; micro-CT; dentistry; dentine; enamel cracks

1. INTRODUCTION

X-ray microtomography (XMT or micro-CT) is most often used as a tool for visualizing structural details in 3D. In studies of *ex vivo* teeth, it is possible to easily discriminate between dentine and enamel, to visualize lesions of various types, and to visualize root canal morphology¹. For quantitative (densitometric) measurements of mineral concentration, it is necessary to have an absolute value of the linear attenuation coefficient (LAC) at each voxel. This requires some form of beam-hardening correction and calibration when using a polychromatic X-ray source. The method used here employs a calibration carousel that is scanned at the end of every specimen scan, in order to record the attenuation of a number of test pieces². These measurements are used in the optimization of a model of the X-ray spectrum, and this model is in turn used to generate a linearization transform based on the known composition of the specimen. For dental specimens, the mineral (which dominates the X-ray attenuation) is assumed to be calcium hydroxyapatite. Where the specimen is immersed (in order to maintain hydration) the method of 2D beam-hardening correction is used to compensate for the immersion liquid and container³. It should be noted that using a more generic method of beam hardening correction, whereby one or more arbitrary parameters are adjusted to give a uniform density across the specimen, cannot be meaningfully applied to tooth specimens due to actual physical gradients in the mineral concentration. Thus, for example, it is not possible, without prior knowledge, to determine whether observed “cupping” of the mineral concentration in enamel is a true representation of higher concentration towards the periphery, or whether it is simply the manifestation of uncorrected beam-hardening.

Generally speaking, the signal-to-noise (SNR or contrast) ratio in XMT is limited by the number of X-ray photons detected. With increasing flux and, or exposure time comes increasing SNR, but an upper limit is imposed by inhomogeneity in the detector array. This may be slight differences in the detector element sensitivities or linearities, or

granularity in the scintillator. In typical XMT arrangements with an effective circular source locus, this gives rise to ring artefacts. These can be “processed out” either before or after reconstruction, or may be reduced by moving the camera between projections. Helical scanning is not so subject to ring artefacts, but even if detector inhomogeneities are not manifest as ring artefacts, they will, at best, contribute to random noise and limit the SNR. Fourth generation medical scanners overcome this problem by using a ring of detectors such that each projection effectively has its apex at a single detector element. The MuCAT scanners designed at Queen Mary University of London achieve a similar end by using a moving camera with time-delay integration (TDI) readout. When first introduced, this system was quite revolutionary in terms of its ability to produce very high quality (SNR) images. However, TDI can only be implemented with CCD detectors, relying on the transfer of charge along the device. Such readout is not possible with flat-panel detectors, which are much more efficient due to their larger size (the scintillator can be made much thicker and they are simply moved further from the specimen to give the same effective resolution). Thus, the CCD TDI systems are less efficient (requiring longer scan times) than modern flat panel systems, but will still yield superior results given sufficient time. They are thus best suited only to applications where high contrast ratio or accurate densitometry is required. Here, an overview of some of the applications in the study of dental hard tissue is presented.

2. METHODOLOGY

2.1 Refinements to beam-hardening correction

As stated previously³, the physics based model used for beam-hardening correction had been replaced with a phenomenological one, whereby the spectrum was modelled as a number of arbitrary intensities at energies from 10 to 90 % of the X-ray voltage, and whose magnitudes were optimized using a simplex algorithm⁴ to minimize the difference between the modelled and measured attenuation of the carousel test pieces. Various means of interpolating between the discrete values have been tested including no interpolation (using the discrete values directly), linear interpolation and spline fitting. Linear attenuation was found to give the best fit (minimum attenuation errors), although no reason could be deduced for this. The simplex optimization was based on the log of the intensities to ensure that the intensities themselves could not be negative. Some experimentation was also performed concerning the ideal number of discrete energy points in the spectrum to be modelled. Because attenuation is independent of the absolute X-ray intensity, one energy point in the spectrum is always fixed, so where 6 points had been previously used, there were only 5 degrees of freedom. Although the 6-point model gave a good fit to the measured carousel attenuation, the upper energies were highly correlated, meaning that a very slight shift in the spectrum could make the upper two energies “see-saw.” Reducing the number of points to 5 gave a slightly larger error in the overall fit, but produced more consistent modelled spectra. This produced better results when comparing repeated scans of the same specimen in order to look for small changes in mineralization.

2.2 Alignment

For alignment of 3D images, we use a 7 degree of freedom alignment algorithm which is similar to a published method⁵, in that it bases the alignment on three orthogonal 2D slices selected from the data sets. Rather than using correlation, the measure of alignment is based on the product of the Sobel transforms (edge enhanced) of the slices to be aligned. The 7 degrees of freedom can be manually adjusted to find an approximate alignment and then refined automatically using a simplex optimization algorithm. An advantage of this is that the edges in the Sobel transform are independent of gradient direction. This is advantageous when the edges change in polarity between the scans to be aligned. An example of this is when aligning filled and unfilled cavities, where the boundary of a void in one image is to be aligned with a filling material with higher X-ray attenuation than the surrounding hard tissue.

2.3 Equalization

With the carousel beam-hardening correction and calibration methodology, repeatability (in terms of the measured linear attenuation coefficient) is typically around 1 %⁶. When looking for small changes in mineralization in successive scans, the relative repeatability error may need to be reduced. In this case, an equalization process is used. One scan (typically the first) in a sequence of scans is used as the reference. Using in-house Tomview software, a series of tags (3D

coordinate markers) are placed at a number of stable regions in the scan, that is, regions where no change in the linear attenuation coefficient is expected in successive scans. For each defined tag, the mean LAC is calculated within a 3-voxel radius and the overall mean for every tag is computed to produce a reference value. Subsequent scans are accurately aligned with the reference scan and the mean LAC calculated from the same tagged coordinates. This is used to generate a correction factor by which the LAC of the entire volume is multiplied in order to equalize it with the reference volume.

3. EXAMPLES OF HIGH CONTRAST XMT IN DENTISTRY

When teeth are subjected to a variety of insults (e.g., decay, abrasion, cracking) there is normally a corresponding pulpal response. This takes the form of reactionary or reparative dentine forming in the pulp, and a slight increase in the mineral concentration following along the path of the dentinal tubules between the pulp and the insult. This increase in mineralization may be due to an increase in peritubular dentine (dentine lining the wall of the tubules) or to sclerotic dentine (complete in-filling of the tubules). Although these features can be seen very clearly using optical microscopy of cut sections, their presence prior to sectioning cannot be determined and without a full 3D data set it is difficult, or impossible, to relate the insult to the reaction. Conventional XMT with limited contrast resolution is often not sufficient to resolve the slight differences in mineral concentration in the dentine, but these are clearly visible with the increased contrast capability of the MuCAT scanner. All teeth referred to were taken from a bank of anonymized extracted teeth in accordance with ethical approval obtained from the Queen Mary Research Ethics Committee (QMREC2008/57).

3.1 Pulpal reaction to enamel cracks

In a study of pulpal responses to enamel cracks, extracted teeth were first screened using XMT for enamel cracks that did not penetrate into dentine and which had the telltale sign of dentine hypermineralisation to indicate that the crack had been present some time prior to extraction. One of these teeth, an upper right first molar, was then embedded in preparation for scanning electron microscopy (SEM). Prior to SEM, a high contrast XMT scan was made. The X-ray voltage was set to 90 kV and current to 180 μ A. The voxel size was set to 15 μ m and 1305 projections were collected over a 24 hour period. Figure 1a shows a rendered view of the reconstructed image (using Drishti from the Australian National University). This tooth has a number of cracks, one of which is arrowed in Figure 1b, c and d. The first of these (b) shows a vertical slice through the reconstructed volume at standard contrast. In Figure 1c, the contrast has been increased by a factor of 8 and the brightness adjusted to show the enamel, allowing the crack to be seen clearly. Note that at the bottom of the image there are beam-hardening/cone-beam artefacts. The reason for this is that the crown of the tooth was close to the flat face of the embedding cylinder and some X-ray paths passed through this face. The modelled cylinder³, however, was continuous, causing the wrong correction to be applied in this region. The gradient seen in the enamel is probably a true reflection of the real gradient in the mineral concentration. In Figure 1d, again with $\times 8$ contrast, the brightness has been adjusted to show the dentine. Here, it is possible to see a streak of hypermineralization through the dentine, from the pulp to the enamel crack. Scanning electron microscopy showed the tubules in this 'streak' were occluded with peritubular dentine. The high contrast images show the subtle variations in local dentine mineral concentration. Further studies on these images are currently being performed, using the high contrast XMT to guide sectioning for SEM and correlating local changes in mineral concentration with microscopic structure.

3.2 Pulp stones

Pulp stones are often seen in XMT images of teeth and in many cases, are associated with dental insult. The tooth shown in Figure 2 was extracted because of severe decay and infection. The radiograph suggested that the pulp was almost completely obliterated by one or more pulp stones. The XMT scanning parameters were the same as above, but the exposure was doubled, so that the scan time was 48 hours. Note, such long exposures are not normally used, but this was to test contrast resolution. In this case, the tooth was not embedded, but scanned in 70 % ethanol. The 'pulp stone' appears to be some form

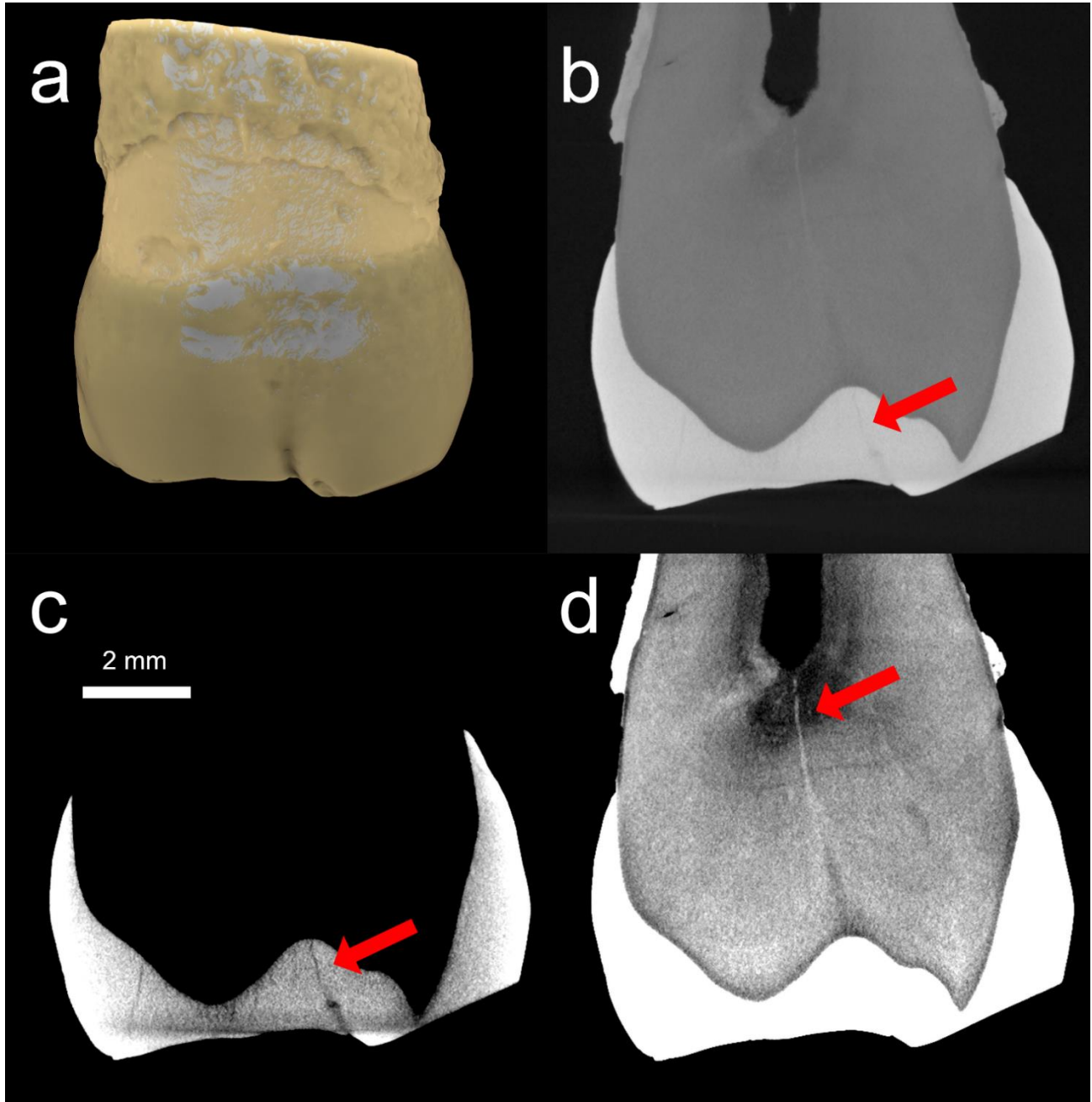


Figure 1: XMT images of an extracted upper right first molar tooth. (a) Rendered with Drishti. (b) Vertical slice through reconstructed volume with standard contrast. (c) Same slice as b, but with contrast increased by a factor of 8 and brightness adjusted to reveal enamel detail. (d) Same slice as b and c, with $\times 8$ contrast increase and brightness adjusted to show detail in the dentine.

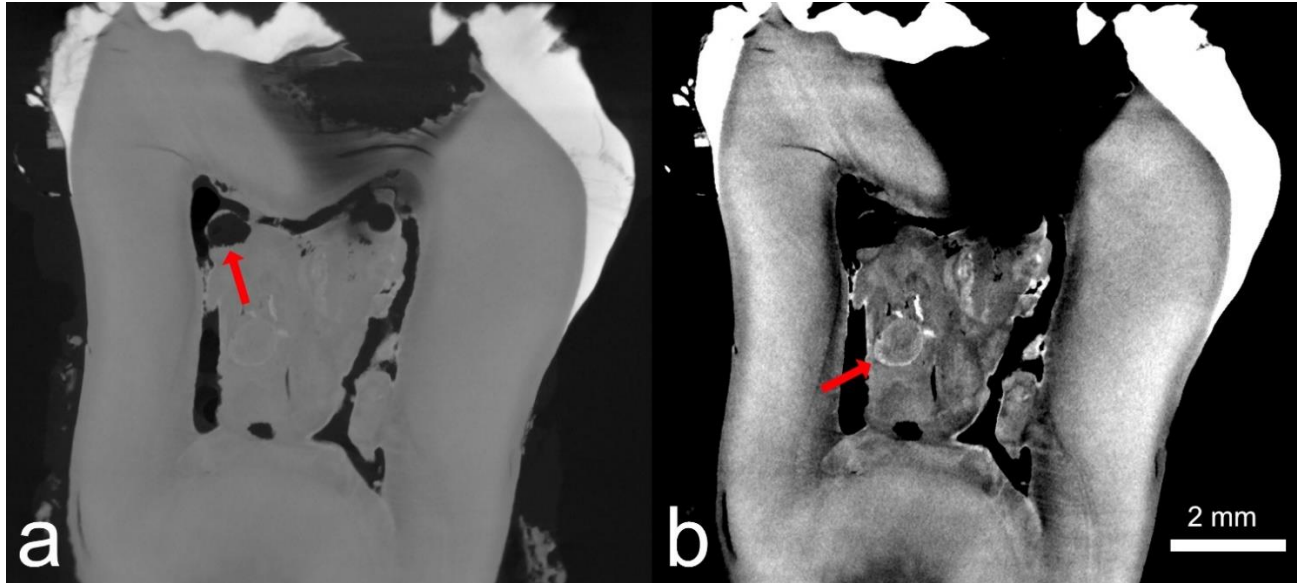


Figure 2: Vertical slice through extracted tooth thought to contain one or more pulp stones; showing reactionary or reparative dentine almost obliterating the pulp. Normal contrast (a) and $\times 8$ contrast (b). Arrow (a) shows possible resorption and (b) encapsulated pulp stone.

of reparative or reactive dentine, yet contains regions where the mineral concentration is much higher than that of dentine. The $\times 8$ contrast image (Figure 2b) shows a wealth of structural detail in the mineral concentration, both in the so called 'pulp stone' and in the surrounding dentine. The feathered edge of the hole seen in the top left of the image (Figure 2a) is indicative of resorption, but this would be very unusual within the pulp chamber. The globular region indicated in Figure 2b is most likely a true pulp stone that has become embedded in reactionary or reparative dentine. Further analysis, including SEM, will be necessary to identify possible causes for these mineralization abnormalities.

The second example of pulp stones is shown in Figure 3. This is a primary tooth with dentinogenesis imperfecta; a condition affecting the formation of dentine and its attachment to enamel. In this condition, the pulp chamber is initially oversized, but gradually reduces down to nothing as dentine continues to form. Several primary teeth had to be extracted from the same patient due to structural damage. XMT images of many of the teeth showed the presence of pulp stones, which were completely isolated from the dentine; others were partially embedded in the dentine. Being a smaller tooth, the X-ray voltage was reduced to 50 kV to increase contrast, and the current was set to 325 μA . The voxel size was 10 μm ; 1215 projections were taken over 16 hours. Note that the signal-to-noise ratio here is reduced because of the increase in resolution. The XMT images showed that the mineral distribution in the dentine is very uniform compared with normal teeth. A partially embedded pulp stone is seen in Figure 3a, its full shape being revealed in the $\times 8$ contrast image in Figure 3b. The enhanced contrast also reveals two further pulp stones that have become completely embedded in the dentine.

3.3 Developing tooth

Figure 4 shows a vertical slice through a developing primary molar. This was an archaeological specimen. It was scanned at 40 kV and 405 μA . The voxel size was 10 μm ; 1107 projections being acquired over 7 hours. It is immediately apparent that the enamel has not matured and that the high organic component in the enamel has caused it to crack extensively as the tooth dried out. A growth line is indicated in Figure 4a, representing a period of disrupted mineralization. This is most likely due to a period of illness. This fault in mineralization has in places caused the enamel to crack at this point, leading to loss of the

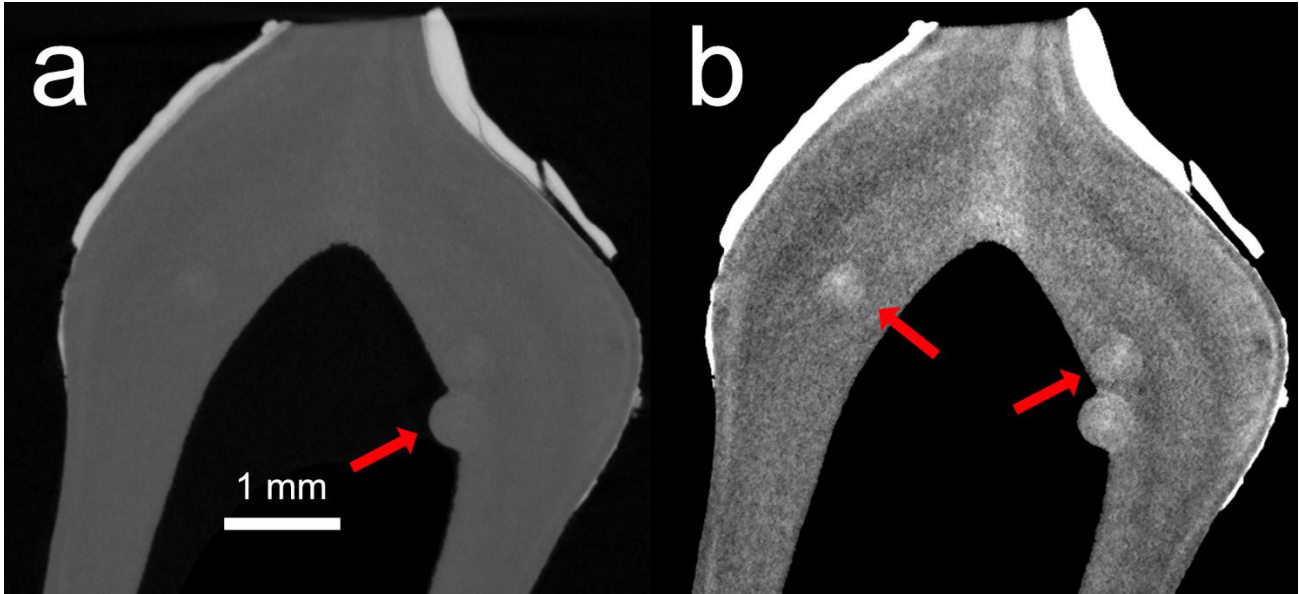


Figure 3: Primary tooth with dentinogenesis imperfecta. A partially embedded pulp stone is indicated in (a) and two fully embedded pulpstones in (b) with $\times 8$ contrast.

enamel. The line is more clearly seen in Figure 4b, where the contrast has been increased by a factor of 4. The large variation in mineral concentration, however, means that the brightness must be constantly adjusted to trace the path of this line at this level of contrast. Such growth lines are visible with light microscopy, but the advantage here is that the possibility exists to trace it in 3 dimensions and thus reproduce the shape of the tooth at the time of the disruption. In samples where there are several such growth lines, it would may be possible to reproduce the shape of the tooth at various times in its development.

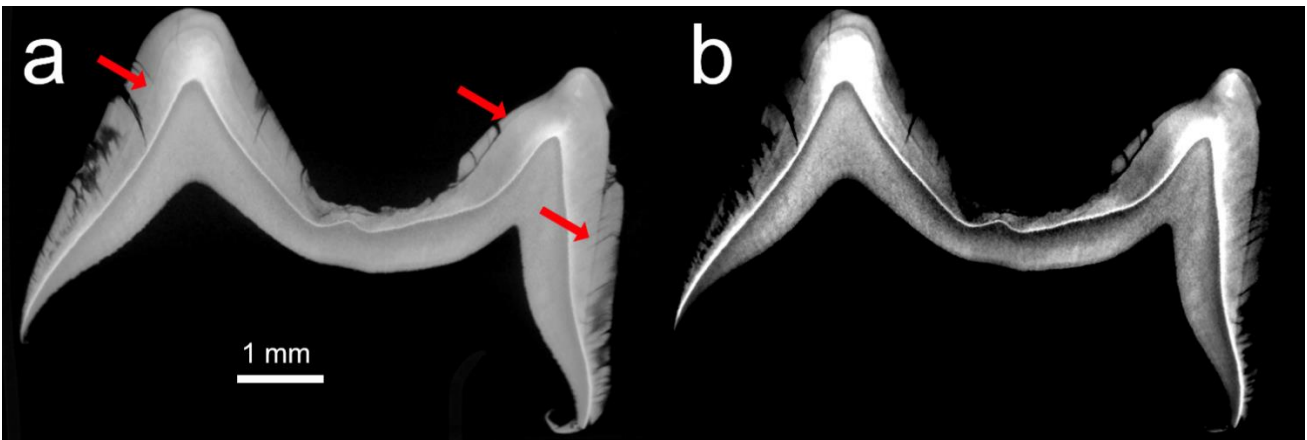


Figure 4: Developing primary molar. A growth line is indicated in (a). Contrast is increased by a factor of 4 in (b).

3.4 Ion release from composite dental cement.

The final example is from a study of ion release from a dental cement, consisting of a composite of an experimental bioglass and resin. The bioglass is designed to release calcium and other ions in order to promote remineralization in demineralized dentine. This experiment draws on all the advances made in high contrast XMT (TDI camera, 2D beam-hardening and calibration, alignment and equalization) in order to identify ion transfer. An extracted tooth with severe caries was excavated with a hand tool, leaving a small region of demineralized dentine to prevent exposure of the pulp. The roots of the tooth were cut off to allow exposure of the pulp to simulated body fluid (SBF). The tooth was glued into a plastic cylinder, open at both ends, with two small blobs of glue applied through holes in the cylinder. This was placed and fixed into a plastic container filled with SBF for scanning. The voltage was set to 90 kV and current to 180 μ A. The voxel size was 15 μ m; 1107 projections were recorded over 20 hours. The cylinder containing the tooth was then placed in a large container of SBF, which was kept in a shaking incubator at 37 °C for 28 days, after which a second scan was performed. A horizontal slice through the filled tooth is seen in Figure 5a. Note, in this preliminary experiment, the bioglass was insufficiently ground, causing large particles to be seen. After alignment, the second scan was equalized with the first (see Section 2.3), requiring adjustment for a 0.9 % difference in the reference values (note to avoid loss of resolution during alignment, a $\times 2$ magnification was performed during reconstruction and the volume was then reduced in size during the alignment procedure). The original reconstruction was then subtracted from the equalized reconstruction of the 28-day scan. The result (with $\times 8$ contrast) is shown in Figure 5b. Here, mid grey represents zero difference, darker levels being negative differences and lighter positive. The very bright regions are where air-filled voids in the first scan have become partially or fully filled with SBF in the second scan. Light and dark outlines around the enamel represent very slight misalignment (less than one tenth of a voxel). This may be a limitation of the alignment procedure, or could be due to dimensional changes in the tooth, brought about by the long period of immersion or change in size of the filling. Of note is the faint, light halo in the dentine around the filling material, representing an increase in the concentration of mineral. The amount of increase varies from around 1 to 2 % of the concentration of sound dentine, showing that the method is capable of detecting very small changes in mineralization. It is not possible, from the XMT, to determine whether the calcium is forming mineral, or whether it is still in ionic form, but it is certain that calcium has been released from the cement into the demineralized dentine.

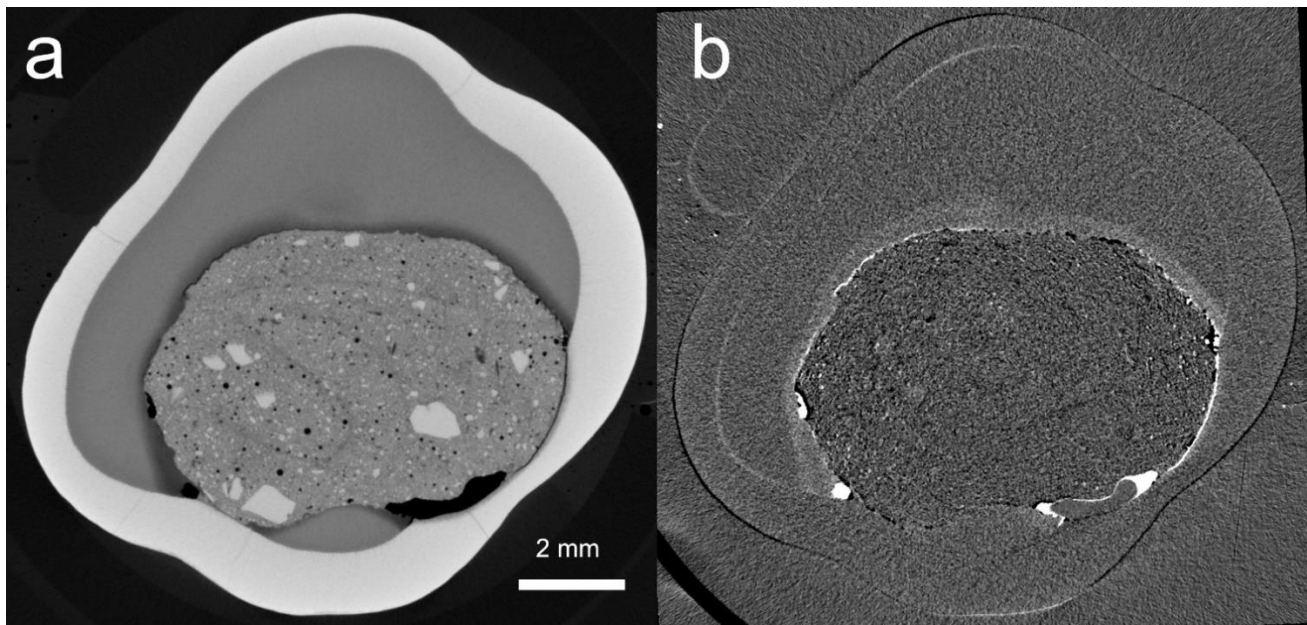


Figure 5: Ion release from composite dental cement. A scan taken immediately after filling is shown in (a). The difference between this scan and one taken 28 days later, with $\times 8$ contrast, is shown in (b).

5. CONCLUSION

The simple concept of using long X-ray exposure to obtain high contrast XMT images has been referred to as “brute force absorption contrast”⁷. The implementation of this principle is not so simple, however, as increasing contrast means increasing susceptibility to systematic errors and artefacts. The methodology has been slowly refined, especially in the area of beam-hardening correction, and good results are being achieved; yet there is still much to do. Further work is necessary on the parametric definition of the modelled X-ray spectrum, one possibility being to define the general shape of the curve with 3 parameters and one further parameter to specify the height of a single emission line. Some experimental work has been carried out on compensation for afterglow and its effect on TDI imaging and also on measuring and compensating for scatter, but to date this has not resulted in improvements in absolute accuracy. Use of a helical or other source locus could also be used to eliminate cone-beam artefacts, but this would have to be weighed against an increase in what is already a very long scan time. Overall, the method has proved to be a useful tool in certain areas of dental research and is aiding in the development and testing of dental materials and techniques.

Acknowledgements

The specimen illustrated in Figure 5 was prepared by Gehong Sun, as part of her MSc in Oral Biology project at Queen Mary University of London.

REFERENCES

- [1] Swain, M. V., and Xue, J., “State of the Art of Micro-CT Applications in Dental Research,” *International Journal of Oral Science*, 1(4), 177-188 (2009).
- [2] Evershed, A. N. Z., Mills, D., and Davis, G. R., “Multi-species Beam Hardening Calibration Device for X-ray Microtomography,” *Proc SPIE*, 8506, 85061N (2012).
- [3] Davis, G., and Mills, D., “2D beam hardening correction for micro-CT of immersed hard tissue,” *Developments in X-Ray Tomography X*, 9967, 996707, (2016).
- [4] Nelder, J. A., and Mead, R., “A Simplex Method for Function Minimization,” *The Computer Journal*, 7(4), 308-313 (1965).
- [5] Liu, X., Laperre, K., and Sasov, A., “Practical pseudo-3D registration for large tomographic images,” *Developments in X-Ray Tomography IX*, 9212, 921208, (2014).
- [6] Davis, G. R., Evershed, A. N. Z., and Mills, D., “Characterisation of materials: determining density using X-ray microtomography,” *Materials Science and Technology*, 31(2), 162-166 (2015).
- [7] Davis, G. R., and Mills, D., “Brute force absorption contrast microtomography,” *Developments in X-Ray Tomography IX*, 9212, 92120I, (2014).